

UNCLASSIFIED

AD-A237 845

2

REPORT DOCUMENTATION PAGE

2b. DECLASSIFICATION/DOWNRATING SCHEDULE

JUN 27 1991

4. PERFORMING ORGANIZATION REPORT NUMBER(S)

6a. NAME OF PERFORMING ORGANIZATION
General Physics Corp6b. OFFICE SYMBOL
(If applicable)5. MONITORING ORGANIZATION REPORT NUMBER(S)
ESMC-TR-91-1

6c. ADDRESS (City, State and ZIP Code)

Cape Canaveral Air Force Station, FL

7b. ADDRESS (City, State and ZIP Code)

Eastern Space and Missile Center
Patrick AFB, FL 329258a. NAME OF FUNDING/SPONSORING
ORGANIZATION

ESMC

8b. OFFICE SYMBOL
(If applicable)

SEM

9. PROCUREMENT INSTRUMENT IDENTIFICATION NUMBER

10. SOURCE OF FUNDING NOS.

PROGRAM
ELEMENT NO.PROJECT
NO.TASK
NO.WORK UNIT
NO.

11. TITLE (Include Security Classification)

Pressure Vessel Burst Test Program

12. PERSONAL AUTHOR(S)

Cain, Sharp and Coleman, General Physics Corp; Webb, Bobby L., ESMC

13a. TYPE OF REPORT

Initial Release

13b. TIME COVERED

FROM _____ TO _____

14. DATE OF REPORT (Yr., Mo., Day)

15. PAGE COUNT

9

16. SUPPLEMENTARY NOTATION

17. COSATI CODES

FIELD	GROUP	SUB. GR.

18. SUBJECT TERMS (Continue on reverse if necessary and identify by block number)

Pressure Vessels, Blast Wave, Fragmentation, Pressurization,
Shock Velocities

19. ABSTRACT (Continue on reverse if necessary and identify by block number)

Since the initial paper, several pressure vessels have been burst using pneumatic pressure. Tests were designed to explore burst characteristics and utilized a well instrumented arena. Data trends for current experiments are presented. This paper is the second progress report on the program and addresses: 1) a brief review of current methods for assessing vessel safety and burst parameters, 2) a review of pneumatic burst testing operations and testing results, including a comparison to current methods for burst assessment and 3) a review of the basis for the current test program including planned testing.

20. DISTRIBUTION/AVAILABILITY OF ABSTRACT

UNCLASSIFIED/UNLIMITED SAME AS RPT. DTIC USERS

21. ABSTRACT SECURITY CLASSIFICATION

UNCLASSIFIED

22a. NAME OF RESPONSIBLE INDIVIDUAL

BOBBY L. WEBB

22b. TELEPHONE NUMBER
(Include Area Code)

(407) 494-7077

22c. OFFICE SYMBOL

SEM

SECURITY CLASSIFICATION OF THIS PAGE

ESMC-TR-91-1

**PRESSURE VESSEL BURST TEST PROGRAM:
PROGRESS PAPER NO. 2**

M. CAIN, D. SHARP, M. COLEMAN
GENERAL PHYSICS CORPORATION
CAPE CANAVERAL AFS, FL

B.L. WEBB
DIRECTORATE OF SAFETY
EASTERN SPACE AND MISSILE CENTER

17 JUNE 1991

APPROVED FOR PUBLIC RELEASE;
DISTRIBUTION UNLIMITED

PREPARED FOR
EASTERN SPACE AND MISSILE CENTER (AFSPACECOM)
PATRICK AIR FORCE BASE, FLORIDA 32925

Accession No.	
STIS GRADE	<input checked="" type="checkbox"/>
STIC TAB	<input type="checkbox"/>
Unannounced	<input type="checkbox"/>
Justification	
By _____	
Distribution/	
Availability Codes	
Dist	Avail and/or
	Special
A-1	

AIAA 91-2091

Pressure Vessel Burst Test Program: Progress Paper No. 2

**M. Cain, D. Sharp, M. Coleman
General Physics Corporation
Cape Canaveral AFS, FL**

**AIAA/SAE/ASME/ASEE
27th Joint Propulsion Conference
June 24-26, 1991 / Sacramento, CA**

91-03135



PRESSURE VESSEL BURST TEST PROGRAM: PROGRESS PAPER NO. 2

Maurice R. Cain*, Douglas E. Sharp*, P.E., Michael D. Coleman
General Physics Corporation
Cape Canaveral Air Force Station, Florida

Abstract

An updated progress report is provided on a program developed to study through test and analysis, the characteristics of blast waves and fragmentation generated by ruptured gas filled pressure vessels. The initial paper on this USAF/NASA/General Physics program was presented to the AIAA in July 1990.

Since the initial paper, several pressure vessels have been burst using pneumatic pressure. Tests were designed to explore burst characteristics and utilized a well instrumented arena. Data trends for current experiments are presented.

This paper is the second progress report on the program and addresses: 1) a brief review of current methods for assessing vessel safety and burst parameters, 2) a review of pneumatic burst testing operations and testing results, including a comparison to current methods for burst assessment and 3) a review of the basis for the current test program including planned testing.)

I. Introduction

Pressure vessels are used extensively in both ground and spacecraft applications. Explosive failures of vessels are rare due to precautions normally taken such as following consensus design, fabrication and test codes and standards. Inservice integrity is maintained through monitoring of vessel service conditions and cyclic history. Yet pressure vessels do occasionally fail, releasing significant energy and possible hazardous commodity into the surroundings. Often it is prudent to assess the damage that could result from explosive failure when locating pressure vessels, designing nearby structures and equipment or considering other safety precautions.

A considerable body of data exists on damage and injury due to blast wave and fragmentation, much of it from research using TNT or similar high explosives. However substantially less is known about blast and fragmentation of bursting pressure vessels than of chemical explosions such as TNT¹. Further, current methods documented in standards, handbooks and other references used to quantify expected energy release, blast waves, and fragmentation are inconsistent and vary in results². Accordingly, a pressure

vessel burst test program is being conducted for the USAF - Eastern Space and Missile Center and NASA Headquarters. The program studies the blast wave and fragmentation of bursting gas filled pressure vessels.

II. Energy Release

An explosive rupture of a pressure vessel, where the stored energy is released instantaneously, would create a blast wave (i.e., shockwave) in the surrounding air and propel fragments. The shockwave and fragment characteristics depend on such things as vessel contents, pressure, vessel geometry and breakup mode.

Energy & TNT Equivalency

The explosive energy from the rapid expansion of compressed gas can be determined by application of basic thermodynamic relationships that are a function of pressure, volume, and temperature. The expansion is most often assumed to be isentropic (isothermal, considered applicable by some references, would require that heat be added to the expanding gas). The following equation gives the isentropic energy released by the failure of a vessel containing a volume of ideal gas, V_1 , at a pressure of P_1 . P_2 is the surrounding atmospheric pressure. K is the specific heat ratio:

$$W = \frac{P_1 V_1}{K-1} \left[1 - \left(\frac{P_2}{P_1} \right)^{\frac{K-1}{K}} \right]$$

This equation assumes ideal gas behavior. Ideal gas behavior is considered adequate for most low pressure situations (1500 psi). The ideal gas assumption for high pressure ruptures gives expansion energies that can be unrealistically high. Accurate estimates of available blast energy from high pressure bursts require calculations based on real gas equations of state supported by empirical data, such as the commonly used compressibility factor Z , defined as $Z = P_v/RT$. Since RT/P is the ideal gas specific volume, the compressibility factor may be considered a measure of the ratio of the actual specific volume to ideal gas specific volume ($Z = 1$). A decrease in stored energy due to compressibility becomes appreciable as pressures are increased above 1500 psi.

Using an isentropic real gas relationship, the calculated stored energy in a cubic foot of GN2 at a pressure of 10,000 psi would be 1,952,744 ft lb. A common

*Member AIAA

practice in determining explosive potential of rupturing pressure vessel is to assume the explosive characteristics are what would be generated by a TNT detonation of equivalent energy. (Other high explosives, such as composition B and composition C-4 are used in the test program and their characteristics relative to TNT have been established³. The TNT energy equivalent of the 10,000 psi vessel filled with GN2 is 1.26 lbs TNT equivalent per ft³ of volume using 1.545×10^6 ft lb/lb after Kinney⁴. The TNT equivalent and energy vs pressure for both real and ideal GN2 with isentropic and Isothermal expansion ($W = P_1 V_1 \ln P_1/P_2$) is shown in Figure 1. The real gas curves were approximated by dividing the ideal gas energy by the average Z to the pressure of interest. (The average was found using the integral of the Z vs P curve. Data will be sought for applying first principles.)

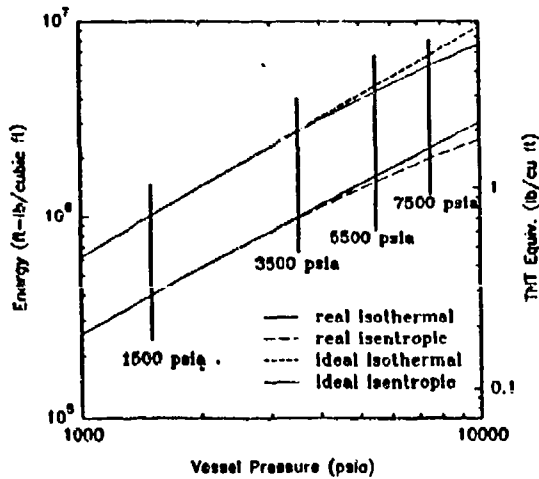


Figure 1. Expansion Energy and TNT Equivalence vs Vessel Pressure for GN2

Blast Waves

Explosive disintegration will generate a blast wave resulting in a high overpressure (pressure above atmospheric) at the vessel surface. As the blast wave advances, the energy is spread over the wave's frontal area, this area increases with the square of the distance from the point of rupture. Overpressure, blast wave velocity and therefore blast effect, decrease rapidly with distance. After passage of the shockwave, the pressure decreases until a suction phase follows in which pressure drops below normal atmospheric pressure. The negative pressure is a result of the outrush of gases from the center of the rupture causing an overexpansion. The pressure above atmospheric at the shockwave front is the peak overpressure and is used with impulse to establish the relative hazard (i.e., shockwave intensity and duration) associated with ruptures and explosions at a given distance. The blast wave emanating from a bursting pressure vessel (Section IV) is somewhat similar to that caused by a high explosive detonation. The pressure close in due to vessel burst is generally lower than high explosive detonation and is a function of burst

pressure. Other variations are caused by vessel and failure geometry and distance from a firm reflecting surface. Figures 2 through 4 show the blast wave characteristics for the detonation of 30 lb of Composition B high explosive that was exploded in an instrumented arena as part of this program (See Sections III and IV). Figure 2 is a plot of pressure vs time at a particular location (90° @ 15') in the arena. Figure 3 is a plot of pressure vs distance for all the arrays in the arena. Figure 4 is a plot of impulse vs distance for the locations shown in Figure 3. The impulse is the area of the positive portion of the pressure-time curve.

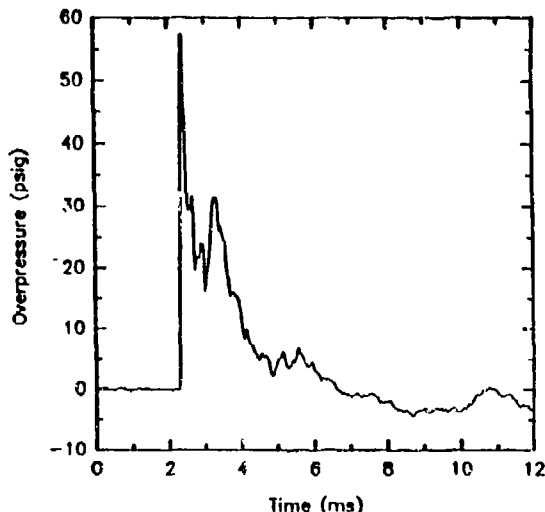


Figure 2. Overpressure vs Time for Composition B at Gauge Location 26 (90° at 15 ft)

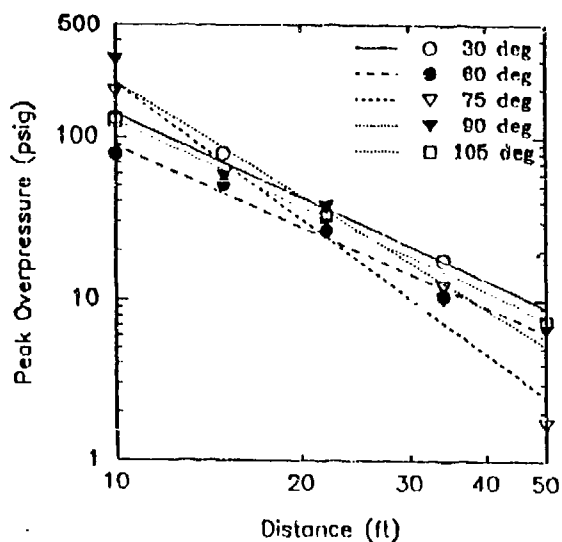


Figure 3. Peak Overpressure vs Distance for Composition B Charge

Fragmentation

The explosive failure of a pressure vessel not only generates a blast wave but produces fragments, with very high velocities possible. Fragments constitute a significant hazard to personnel, systems, components and structures in

the vicinity. Primary fragments are portions of the vessel or its attachments that are accelerated due to the internal pressure of the vessel. Secondary fragments may also be produced due to the action of the blast wave or primary fragments on nearby objects.

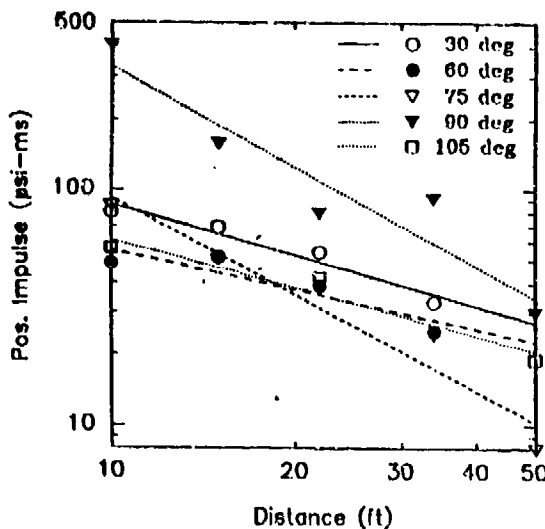


Figure 4, Positive Impulse vs Time for Composition B Charge

Studies^{5,6,7} of the characteristics of vessel fragments has addressed the velocities of fragments produced, their trajectories and, as a result, their ranges and their impact velocities. Determination of the initial velocities of fragments has been undertaken by several researchers. Most such studies are based upon work by Taylor and Price⁸ which predicted the velocities of two spherical vessel fragments accelerated by either an expanding isothermal or adiabatic, ideal gas. Their analysis has been used, extended or modified by several other researchers to improve upon their assumptions or to adapt the analysis to other cases.

Once the initial velocity of a fragment has been determined, its range may be found through ballistic calculations, generally done through the use of a computer code, a number of which are available. Code considerations are drag coefficient, lift coefficient (if any), initial trajectory angle and reference area - either fixed or varying (tumbling or gradually changing).

Experimental determination of fragment velocities was discussed in the initial program paper. The reader is referred to work by Pittman⁹, Jager^{7,10} and Baum⁶ for further information.

III. Test Program

Test Program Matrix

A test program matrix has been developed that includes a series of test plans each with multiple pneumatic vessel bursts. The objective of the program matrix was to

force vessel bursts in such a way as to generate worst case blast waves and fragmentation, such that a model could be developed that would envelop generally expected vessel failures. The latter test plans of the matrix would include such representative vessel failures. Worst case however is a function of several variables, including location and orientation of failure, pressure, vessel shape, fragment type and number and height above ground. The plans and tests comprising the program matrix have been developed to minimize the number of vessel bursts yet meet the stated objective with valid data.

In the development of a test matrix, it was also recognized that a pressure vessel burst may not produce a spherical shockwave as does a TNT explosion. The blast wave from a pressure vessel burst may be much stronger in one direction than another based on how the vessel shell comes apart. To provide a direct experimental comparison with pressure vessel bursts, spherical high explosive detonations will be conducted as part of the test program.

Accordingly, a test program matrix was developed which incorporated varied failure locations and mechanisms. Seven test plans were envisioned with each test plan consisting of several vessel bursts. The failure geometry shown in Figure 5a and b for five of the seven test plans would be accomplished through the use of optimally selected shaped charges and pre-machining of grooves. Test plan four would use shaped charges alone. Test plan seven is intended to produce only one fragment with a side split. The anticipated split will be oriented toward the arena transducer field.

Other burst parameters are also varied in the program matrix. These include the split location, burst pressure and L/D for two fragments and multi-fragment vessels as shown in Figure 5.

Vessel measurements of interest are pre-burst gas pressure and temperature, pressure during the fragment acceleration phase, fragment velocity and blast overpressure. Fragment velocity will be assessed using accelerometers, contact wire strikes and high speed motion picture and video. Blast overpressures will be measured on the ground in a multi-point arena and at height of burst (HOB) at a lesser number of points.

The matrix shows what results are being emphasized for each test plan, however all the tests are interrelated. Other results include TNT equivalency, energy distribution and fragmentation characteristics for TP #7.

Test Planning & Preliminary Testing

Burst Initiation

The use of pre-machined grooves and optimum shaped charges presents several questions to be addressed in the planning stages. The typical groove geometry is shown in Figure 6 with the linear shaped charge (LSC) and the shaped charge cut area shown with dotted lines.

Describing	Test Plan #1	Test Plan #2	Test Plan #3
Vessel:			
Material	Steel	Steel	Steel
Vol., ft^3	53	53	53,22
Diameter, in	24	24	24,16,14
L/Ds	11	11	11,17,24
Burst Pressure	varies	3500	3500
No. of bursts	4	3	4
Configuration			
			
	$\#1: P = 1500$		
	$\#2: P = 1900$		
	$\#3: P = 3500$		
	$\#4: P = 3500$		
Para Varied	Burst pressure	Burst height	L/D-2 frags
Results			
Asymmetries	oburst asymmetry circular vs real gas	reflection factor oburst asymmetry	oburst asymmetry circular velocity reflection factor

Figure 5a: Test Program Matrix

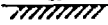
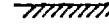
Test Plan #4	Test Plan #5	Test Plan #6	Test Plan #7
Composite	Steel	Steel	Steel
53	53	53,22	53,22
14	24	24,16,31	24,16
1	11	11,17,24	11
4000	2500	3500	7700
4	3	4	4 min
(D)			
			1 burst with each type vessel
			flow or pressure variations to be determined
			
2 each			
vessel shape & orientation	split location	L/D multi-fragment	machined flow
burst asymmetry	burst asymmetry	fragmentation	burst asymmetry
reflection factor	initial velocity	ideal vs. real gas	energy distribution
initial velocity			wave front shape

Figure 5b, Matrix, Continued

Machining such a groove with a constant remaining wall thickness in a vessel of non-uniform roundness and wall thickness presents an interesting challenge. For single circumferential grooves, this challenge was met using a procedure for eight equally spaced offsets of the vessel towards a lathe cutting tool, using a computer supported setup, and swinging a slightly larger radius than the desired and resultant cut. For multi-fragment vessels, having grooves in two directions, Computer Numerical Control milling is indicated.

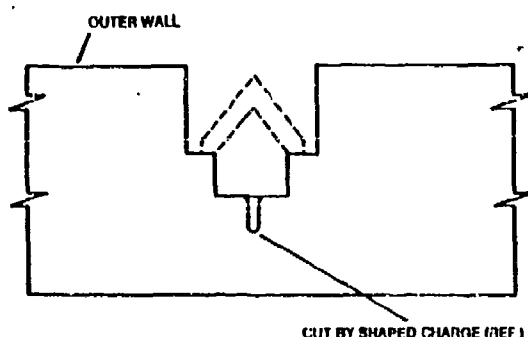


Figure 6. Typical Vessel Cross Section Showing Groove and Shaped Charge.

The typical 2:1, tangential to longitudinal, stress ratio in a cylindrical pressure vessel causes concern regarding the stress environment at a narrow groove, particularly when a failure due to longitudinal stress is desired. This concern led to material tests on a sacrificed vessel and a preliminary hydrostatic burst test. These tests showed that, in a non-cyclic application the tangential stress in a narrow circumferential groove can be used alone to predict failure.

A linear shaped charge is used to cut a groove at the bottom of the machined groove to increase an already high stress level, due to pneumatic pressure, thereby causing failure. The difficulty is selecting a small LSC sufficient to cause failure. A small LSC is desired to reduce the possibility of shaped charge fragments damaging transducers and to reduce the explosive blast wave since the vessel burst blast wave is to be measured. A preliminary LSC/pneumatic burst test was deemed appropriate for 1) finding the detonation cut in the particular vessel material, 2) quantifying an LSC shock effect on a relatively thick wall vessel that would assist the detonation cut in causing failure and 3) quantifying interference of the LSC blast in measuring the blast due to vessel burst. From the latter effect an LSC blast pressure tare subtraction routine was anticipated. The tests showed that any shock effect was minimal and that the LSC blast pressure has practically returned to ambient prior to the vessel blast shock arrival as shown in Figure 7, thus minimizing measurement problems.

Pressurization System

A pressurization system was designed and built for the burst testing. Due to the potential hazard to equipment, the system evolved into the use of a protected and semi-buried storage vessel and a free flow/booster system operated remotely by personnel in a blockhouse shelter. A fragment hazard assessment was conducted using a Taylor-Price⁸ computer code, a ballistics computer code for fragment flight distance and data from Baker⁹ and Moore¹² to predict penetration/protection of the blockhouse.

Instrumentation Ranging

Camera speeds were determined based on calculated fragment velocity. For blast pressure transducer setup and

ranging, the blast pressure expected from a high explosive burst of equivalent energy was used for the first pneumatic burst. This resulted in near-field pressure measurements which were noisy, but useable, due to actual pressures being lower than anticipated. Subsequent ranging of transducers for pneumatic bursts is being adjusted accordingly as described in Section IV.

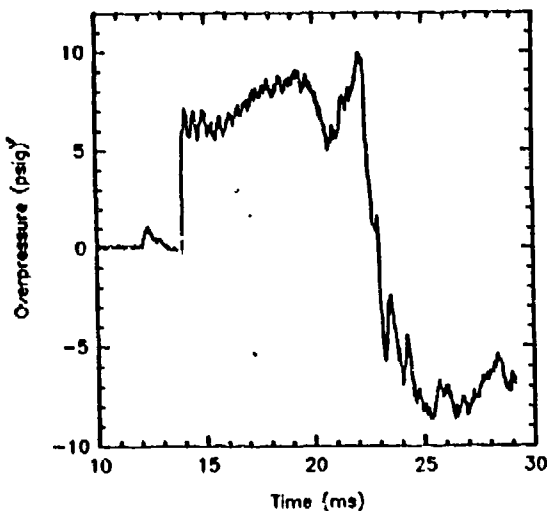


Figure 7, Overpressure vs Time for 3300 psig Vessel at Gauge Location 26 (90° at 15 ft)

Test Site

Pneumatic burst tests have been conducted at the Naval Surface Warfare Center's (NSWC) Dahlgren, VA explosives test area. The Center has personnel experienced in explosive detonation and blast data recording from small up to very large charges of high explosive. High speed motion picture coverage is available with multiple cameras and hardened camera shelters. Heavy duty handling equipment is available such as cranes, fork lifts, pyloaders, etc. A variety of transducers, tape recorders and timing controls are available for testing. A hardened blockhouse and instrumentation room plus the capability of tape recorder control from a remote site is available. This site provides an already wired arena in close proximity to a blockhouse which can prevent penetration of high kinetic energy fragments. An isometric drawing of a pressure vessel installed in a blast field arena at NSWC is shown in Figure 8.

IV. Test Results

Two pressure vessels were burst at 3300 psig and 4750 psig, respectively in the preliminary pneumatic burst test series and three vessels were burst at 1500 psig, 3500 psig and 5500 psig, respectively in an abbreviated execution of Test Plan #1. A fourth vessel burst, planned for 7500 psig in the second test series, was postponed due to a malfunction of the pressurization system. In addition to the

vessel bursts, high explosive (HE) shots were conducted for each test series to check out the instrumentation and to serve as comparison data. This also permits pressure vessel data to be compared to standards such as TNT.

For each of the vessel bursts and HE shots, pressure was recorded at between 46 and 51 locations, using mostly transducers flush with the ground surface. Positive impulse was obtained by integrating the pressure time data. For each vessel burst, vessel pressure and internal gas temperature were measured up to the point of burst. Attempts to measure internal vessel pressure decay using the same high response pressure transducer met with limited success. Attempts to measure vessel fragment acceleration using accelerometers were unsuccessful and led to the use of contact wires during the second test series. High speed motion pictures and high speed video were recorded for estimating velocities of vessel halves. Figure 9 shows a frame from high speed video of the 4750 psi burst.

Data is presented and discussed primarily for the 3300 psig vessel burst and for a 30 pound charge of Composition B of about the same TNT energy equivalence as that vessel burst.

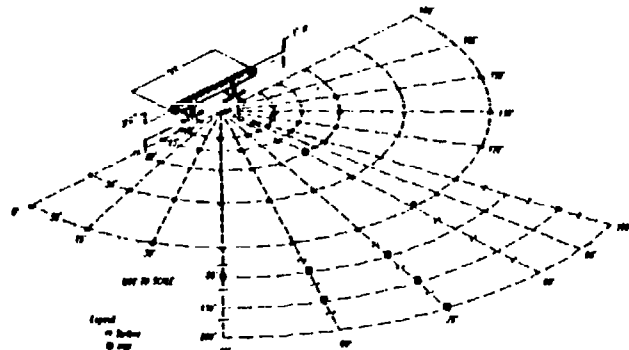


Figure 8, Pressure Vessel Installed in NSWC Arena

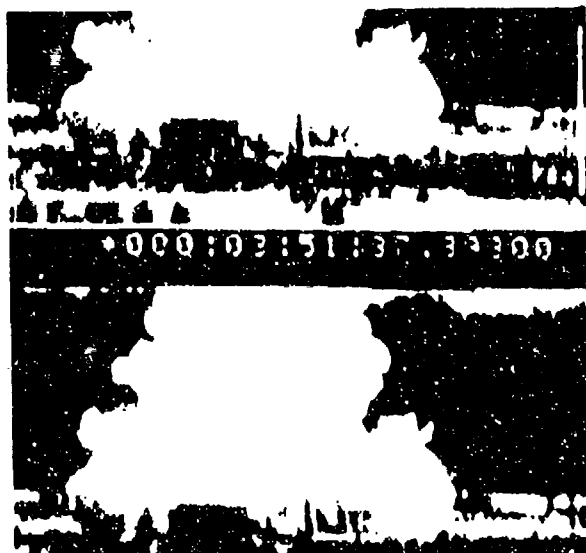


Figure 9, Vessel Burst at 4750 psig, from High Speed Video

Field Overpressure

The pressure vs time response of a typical ground-flush transducer is shown in Figure 7. For comparison, this is the same transducer (reranged) and location as used for Comp B overpressure shown in Figure 2. The initial small pressure increase is due to detonation of the shaped charge. Pressure has decayed to zero before the vessel blast reaches the transducer. Rather than the sharp pressure rise and rapid, exponential decay characteristic of a high explosive (HE) blast, pressure increases to a peak value and remains approximately constant for 8 ms. Subsequent decay is slower than that from a HE blast.

The peak overpressure recorded at each transducer location is plotted vs distance for five arrays (identified in Figure 8) of the 3300 psig vessel burst in Figure 10. The data points shown are the peak overpressures recorded at transducer locations. The lines are the best log-log curve fit for each of the arrays. Overpressures are higher for the arrays approaching normal to the vessel than for arrays approaching parallel to the vessel axis due to jetting of gas along the 90° array (vessel center). This asymmetric pressure variation was especially noticeable close-in to the vessel.

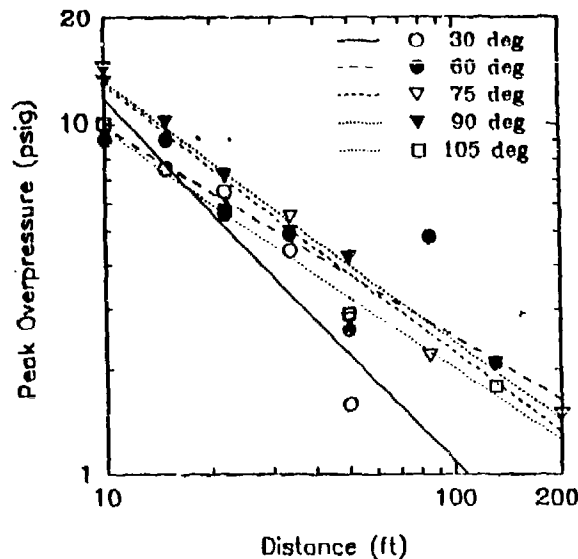


Figure 10, Peak Overpressure vs Distance for 3300 psig Vessel Burst

Figure 10, pressure vessel overpressures, may be compared to Figure 3, the approximate energy equivalent high explosive shot. The vessel near field overpressures are seen to be less and those for the far field greater than Comp B. Overpressures in Figure 3 are expected to be symmetric for an HE blast.

Overpressures in the 90° array are plotted vs distance in Figure 11 and superimposed over expected pressure-distance curves for 5 different charge weights of TNT. The 5 charge weights chosen are those that would yield the

overpressures measured from the vessel burst at the transducer distances. The TNT overpressure vs distance curves are from a functional relationship for chemical explosions in Kinney & Graham⁴. It is seen that in the near field (10' distance) the measured overpressures from the vessel burst are the same as would be measured from a small charge weight TNT blast. But in the far field, (50' distance), the magnitude of the measured overpressures are equivalent to that produced by a large charge weight TNT blast. The TNT energy equivalence of this vessel was 31.6 pounds. Similar results were obtained for the other arrays.

Impulse

Positive impulse measured during the 3300 psig vessel burst is plotted vs distance for 5 arrays in Figure 12. This figure may be compared to the impulse data shown in Figure 4 for the approximate energy equivalent Comp B high explosive shot.

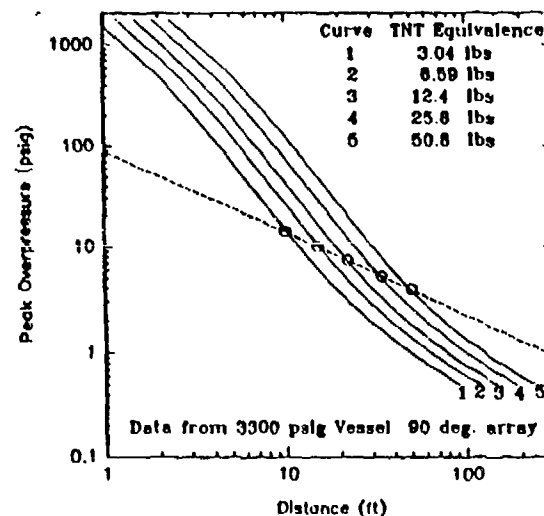


Figure 11, Peak Overpressure vs Distance Contours for Different TNT Equivalences

Also plotted in Figure 12 are lines showing the expected impulses from various values of TNT explosions, taken from a function for chemical explosions in Kinney & Graham⁴. This may also be compared to the #30 Comp B blast, Figure 4, which has a TNT equivalent for impulse of 28 pounds.

Arrays in Figure 12 which are nearly normal to the vessel axis (75°, 90°, 105°) produce impulses greater than expected for the equivalent energy TNT charge while arrays nearly parallel to the vessel axis (30°) produce impulses less than expected for the equivalent energy TNT charge. The 3300 psig vessel burst impulses exceeded those expected from Comp B nearly normal to the vessel axis but were less than that from Comp B nearly parallel to the vessel axis, again due to jetting effect. This approximately supports the expectation of Held et al¹¹ that a pressure vessel burst has the same impulse as a high explosive blast of the same energy equivalence.

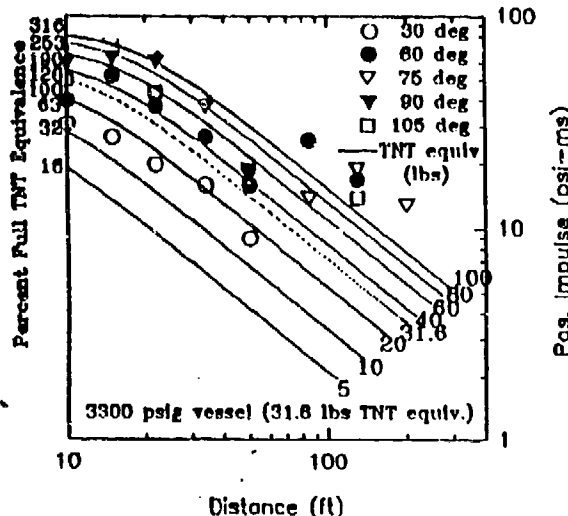


Figure 12. Positive Impulse vs Distance Contours 3300 psig Vessel Bursi (31.65 lbs TNT equivalence)

Fragment Velocities

Velocities of vessel fragments (halves) were estimated from films or high speed video taken of the vessel bursts. The velocity of the fragment connected to the fill tubing was slightly less than its opposing end due to the work required to drag and deflect the tubing. (The tubing breaks between the vessel and an anchor point after full velocity has been achieved.) Velocity of the unhindered half of the vessel, after initial acceleration, is shown for each vessel in Table 1. Fragment velocities were compared to predictions made by a code based upon the Taylor-Price analysis⁶. It was found that by modifying the discharge coefficient, k , (of the area between the fragments) the code full velocity could be matched to the measured velocity. Table 1 also summarizes the discharge coefficient required to match the measured velocity.

Table 1
Comparison Between Measured and Calculated Velocities

Vessel Pressure (psig)	Measured Velocity (ft/s)	Discharge Coefficient, k
3300	246	0.41
4750	306	0.43
1500	148	0.44
3500	250	0.46
5500	315	0.55

For vessels #1 and #3 of Test Plan #1 (1500 and 5500 psi respectively) wire contact times were measured as a sharp edge attached to the vessel passed through wires on a close proximity breakwire frame. Tables II and III compare the average velocities during the one foot intervals for the measured data and for calculated positions using $k = .6$ and the Taylor-Price code.

Table II
Vessel #1 - 1500 psig

Distance: from → to	average velocity (ft/sec)	
	measured	calculated
.448' → 1.448'	104.0	103.1
1.448' → 2.448'	129.7	126.5
2.448' → 3.448'	148.1	132.4

Table III
Vessel #3 - 5500 psig

Distance: from → to	average velocity (ft/sec)	
	measured	calculated
.750' → 1.750'	220.8	230.8
1.750' → 2.750'	247.5	276.2
2.750' → 3.750'	275.5	294.5

The reason for the calculated velocities to be underestimated at 1500 psig and overestimated at 5500 psig is unclear. An increase in the discharge coefficient, k , has an inverse effect on calculated velocities due to the increased flow normal to the fragment flight direction. A value of $k = .44$ for the 1500 psig case and $k = .8$ for the 5500 psig case produces close results for lines one and three of both tables, although the center position of both tables is overpredicted.

Shock Velocities

Average shock velocities between transducer positions on an array were found from delta arrival times for PV #2 (3300 ps^{-1}) and PV #3 (4750 psi) of the preliminary test. The velocity between 10 and 15 feet for both bursts was a maximum of 1430 feet per second (FPS). The velocity generally diminished with distance for each case and was 1150 FPS between 130 and 200 feet on the 75° array for the 4750 psi case.

Figure 13 is a plot of average shock velocity between points vs peak overpressure at the downstream point for both 3300 and 4750 psi pressure vessels noted above. Superimposed over the vessel data is a curve illustrating the functional relationship between shock velocity and overpressure from Swisdak³ at a temperature of 84°F (the average of the ambient temperatures for the two vessel bursts). The data trend is to follow the curve with more scatter in evidence for the PV #3 burst than the PV #2. (Instrumentation for the PV #2 burst was better ranged as discussed in Section III.) A statistical error analysis showed that the PV #2 data fit the curve twice as good as PV #3 which had an error deviation, S_e , of 2.9 psig.

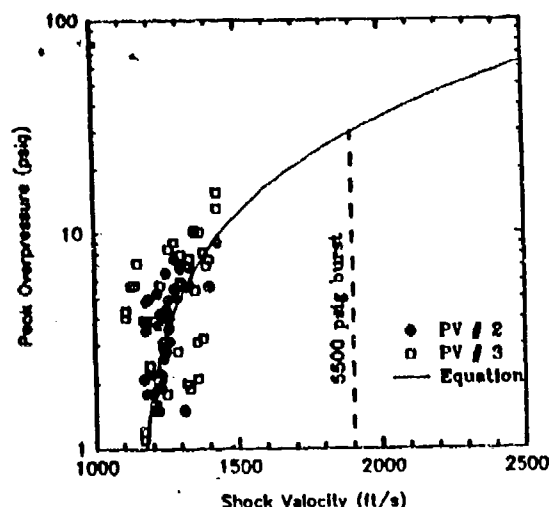


Figure 13, Peak Overpressure vs Shock Velocity

For the 5500 psi burst of TP #1 an attempt was made to measure pressure at eight inches from the vessel surface and on the ground 2 1/2 feet below the vessel surface. Arrival times were measured for both but the setup for the 6 inch distance transducer was blown away during the pressure rise time. The transducer at 2 1/2 feet experienced a gradual pressure increase to 310 psi. The difference in arrival times provides an average velocity of 1900 FPS between the two points, also shown on Figure 13. This velocity would seem to indicate a low average pressure between the two points which is not substantiated by the ground mounted transducer.

V. Future Efforts

Problems with the pressurization system will be corrected. The one remaining burst in Test Plan #1 will be conducted during Test Plan #2. Data will then be available for a burst pressure range of 5 to 1.

An attempt will be made to nondimensionalize the pressure data to coefficient form. Preliminary indications are that this may be possible by dividing the overpressure in absolute units by the maximum shock pressure expected, Held et al¹¹. The maximum shock pressure is from the one dimensional flow shock tube equation applied to the three dimensional vessel burst. This may only apply to 10 feet away and farther until additional ground reflection data close to the vessel is obtained (TP #2). Maximum initial shock overpressure (shock tube equation) expected is 145 psi for the 7500 psi vessel without considering reflection. A pressure of 310 psi was measured under the 5500 psi vessel.

An attempt will be made to look for real gas effects although these may be somewhat small up to 7500 psi as depicted in Figure 3. Ideally, tests should be conducted at pressures as high as 15,000 psig in order to assess real gas effects. This was not considered due to pressurization system and vessel costs and the more limited applicability of such data.

Test Plan #2 will provide blast field pressure variations with height of burst. Additionally close pressure measurement will be sought in the absence of a close ground surface to complement the data obtained in Test Plan #1.

Test Plans #3 (dual fragment) and #6 (multifragment) will each vary the vessel length to diameter ratio (L/D). Figure 14 shows the calculated vessel energy remaining as a function of time, shown as a percent of the energy at 3500 psi burst for five vessels and failure geometries. Four of the curves are for a 22 cubic foot vessel which shows a large variation with L/D from 16 inch diameter vessels to 34 inch diameter vessels. The other curve applies to the 53 cubic foot, 24 inch diameter burst at 3500 psi (Test Plan #2). The escape rate of the vessel energy should effect overpressure measurements and fragment velocity. The two test plans permit approaching the case of sudden disintegration of the pressure vessel walls, an assumption made in some comparisons of vessel burst overpressure to high explosive blast.

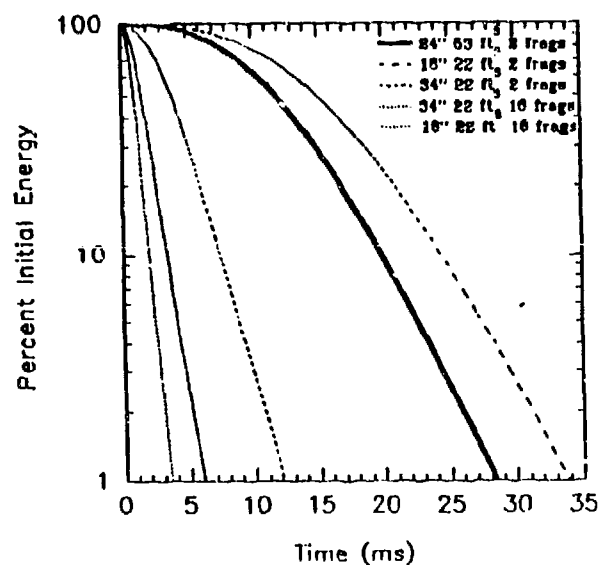


Figure 14, Remaining Vessel Energy vs Time Following Vessel Burst

VI. Summary

A data base exists for estimating injury and damage from blast wave overpressure and impulse and from fragment impact velocity and mass. However much of the

data compares a pressure vessel burst to a high energy explosive blast. Additional vessel burst testing is needed to segment existing data in quantifying pressure vessel burst characteristics. The current test program will provide a mix of vessel failure modes, pressures, and other variables. This data, together with data from other researchers will permit assessing the results of different assumed options for vessel failures such that the installation designer or user can weigh the likelihood of such failures and the hazards should they occur.

This paper is the second progress report on the pressure vessel burst test program. Some pneumatic burst testing has been accomplished and limited conclusions are drawn. Since test plans are interrelated, further testing will clarify existing results and provide conclusions to be presented in the future.

Tentative conclusions are as follows:

- 1.) At close distances, vessel burst overpressures are less than that of high explosive blasts with equivalent energy and are greater than HE far from the vessel. For an example cited, the overpressures due to vessel burst and HE blast were equal at about 40 feet from the vessel.
- 2.) Both the overpressure and impulse data are very directional for a circumferential vessel failure. However, the vessel impulse is approximately equal to the HE impulse along an arc line 50° from the vessel axis at all distances from 10 feet to 50 feet. This approximately supports the conclusion that the impulse is the same for both vessel bursts and equivalent energy HE blasts.
- 3.) The functional relationship between shock velocity and overpressure ratio appears to be the same for vessel bursts as for HE blasts.
- 4.) Fragment velocity may be calculated using a Taylor-Price type code, however the discharge coefficient, k, to use is uncertain and may not be a constant during acceleration. Full velocities (after acceleration) were calculated using $k = .41$ to $.55$. Velocities during acceleration were calculated using $k = .44$ to $.80$.
- 5.) Based on limited data, average shock velocity to 6.1 feet from the vessel surface is less than Mach 2. This, combined with #3 of this summary supports the conclusion that the initial shock overpressure is much less than vessel pressure and may be found using the one dimensional shock tube equation.
- 6.) Dividing the overpressure in absolute units by the initial shock overpressure as predicted by the shock tube equation, appeared to remove all data trends except for distance and array angle for distances of 10 feet to 50 feet. This provides a method for estimating ground overpressures for this particular vessel failure geometry, length to diameter ratio and height of burst.

References

- 1) Brown, S.V., "Energy Release Protection for Pressurized System. Part I - Review of Studies into Blast and Fragmentations," Applied Mech. Review, Vol. 38, No. 12, ASME, December 1985.

²Coleman, M. et al, "A Review of Energy Release Processes From the Failure of Pneumatic Pressure Vessels," ESMC-TR-AB-03, August 1988.

³Swisdak, "Explosion Effects and Properties Part I - Explosion Effects in Air", NSWC/WOL/TR 75-116.30, 1975.

⁴Kinney and Graham, Explosive Shocks in Air, 2nd ed, Springer Verlag, 1985.

⁵Baker, W. et al, "Workbook for Predicting Pressure Wave and Fragment Effects of Exploding Propellant Tanks and Gas Storage Vessels", NASA CR-134906, November, 1975.

⁶Baum, "Disruptive Failure of Pressure Vessels: Preliminary Design Guidelines for Fragment Velocity and the Extent of the Hazard Zone", Transaction of the ASME - Journal of Pressure Vessel Technology, May, 1988.

⁷Held and Jager, "Assessment of Gas Pressure Vessel Burst Hazard", ASME PVP, Volume 62, 1982.

⁸Taylor, T.D. and Price, C.S., "Velocities of Fragments from Bursting Gas Reservoirs", Journal of Engineering for Industry, November, 1971.

⁹Pittman, "Blast and Fragment Hazards from Bursting High Pressure Tanks", Naval Ordnance Laboratory, May, 1972.

¹⁰Jager and Junge, "Measurement of Pressurized-Air Vessel Fragment Velocity", 1981.

¹¹Held, Jager, Stolzl, "TNT Blast-Equivalence for Bursting of Pressurized-Gas Conventional Vessels", 1981.

¹²Moore, "The Design of Barricades for Hazardous Pressure Systems", 1966.

Acknowledgements

The program described is ongoing under the direction of the USAF Eastern Space and Missile Center, and is jointly directed and supported by NASA Headquarters. The program is performed by the Pressure Systems Technology Department of General Physics Corporation and involves the effort of other government centers, subcontractors and suppliers. We would like to thank all for the support and input to the program, especially Mr. Lou Ullian and Mr. Bobby Webb of ESMC and Mr. George Rodney and Mr. Wayne Frazier of NASA Headquarters. We would also like to thank Mr. Kent Rye of the Naval Surface Warfare Center for his diligent efforts and Ms. Susan Hudec of General Physics for typing the paper.